Wide-Area, Carrier-Phase Ambiguity Resolution Using a Tomographic Model of the Ionosphere

OSCAR L. COLOMBO
NASA Goddard Spaceflight Center, Greenbelt, Maryland

MANUEL HERNANDEZ-PAJARES, J. MIGUEL JUAN, and JAUME SANZ
Universitat Politècnica de Catalunya, Barcelona, Spain

Received September 1999; Revised March 2002

ABSTRACT: *A method for resolving GPS carrier-phase ambiguities exactly at hundreds of kilometers from the nearest reference site has been tested under a variety of operating conditions, with help from a computed tomography model of the ionosphere. The objective is decimeter-level (root mean square) wide area kinematic positioning in real time using broadcast orbits, and subdecimeter-level positioning using precise orbits. This work is relevant to surveying and navigation, as well as to newer real-time uses of GPS, such as monitoring of atmospheric water vapor. The paper shows how this objective could be achieved using GPS data from a wide area network to obtain a regional ionospheric model. Information from the model would then be transmitted to users so they could apply precise ionospheric corrections to their data at the approximately known locations of their rovers. Test results are summarized, including detailed results of one test involving a large-area network and an active ionosphere.*

INTRODUCTION

In the Wide Area Augmentation Systems (WAAS) [1], GPS pseudorange data are used to position aircraft in real time, with meter-level precision, relative to reference stations hundreds of kilometers away. With the same reference stations but using the more precise carrier-phase measurements instead of pseudorange, one could, in principle, obtain subdecimeter precision. Although phase measurements are ambiguous, it is possible to resolve their ambiguities exactly. Indeed, this ambiguity resolution has been the subject of numerous studies since the mid-1980s, many of them published in this journal. Yet the fast and reliable resolution needed for navigation is hindered by differences in the amount of ionospheric refraction experienced by satellite radio signals on their way to places on earth separated by more than 10–20 km. This distance limit grows shorter as the ionosphere becomes denser and more agitated with an increase in solar activity, as it is occurring now, near solar maximum. Figure 1 shows how such activity (closely linked to the number of sunspots) is expected to remain high for several years past the present peak.

Real-time resolution of ambiguities over much longer distances would improve surveying, navigation, remote sensing, and surveillance over large areas, in the last two cases by allowing more accurate sensor geolocation (e.g., for radar and digital cameras) and sensor orientation (using inertial units calibrated with precise position updates). New GPS applications, such as real-time wide area monitoring of water vapor in the atmosphere, would become practicable.

One alternative to fixing the ambiguities over long baselines is to "float" them, essentially treating them as real-valued unknowns in the observation equations. When using this approach, however, the position estimated with a navigation Kalman filter typically takes more than 30 min to attain high precision—too slow for many applications. Fortunately, it may be possible to resolve the carrier-phase ambiguities on the fly (OTF) and so achieve high precision, in a matter of minutes, over distances of hundreds of kilometers between rover and reference stations, using double-differenced data corrected with a suitable ionospheric model [2, 3]. Very precise corrections can be made using data from a network of permanent control stations with dual-frequency receivers. The corrections can be based on different types of ionosphere models [4–10]. In our own work [11–16] we use a two-layer tomographic model. This model has been shown (e.g., in [6]) to provide fast and accurate estimates of total electron content (TEC) under conditions of high electron density variability, such as those close to the geomagnetic equator, during solar maximum.

NAVIGATION: *Journal of The Institute of Navigation*
Vol. 49, No. 1, Spring 2002
Printed in the U.S.A.

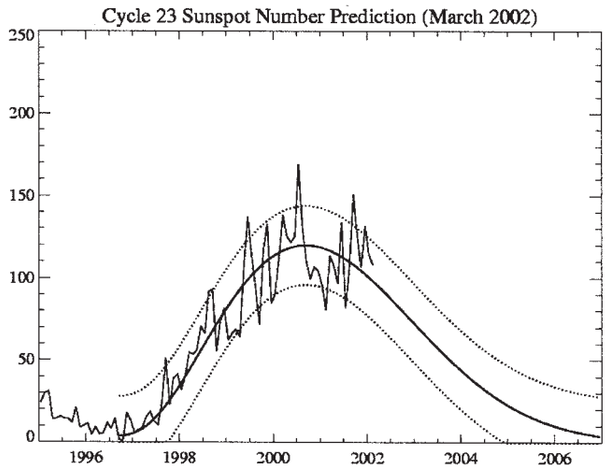

Fig. 1–Sunspot Number for Current Solar Cycle, Predicted and Measured

REAL-TIME, WIDE-AREA TOMOGRAPHY

The flow chart in Figure 2 shows the steps taken to obtain the double-differenced ionosphere corrections for the rover GPS receiver. There are three main steps:

Step 1—The ionospheric model is created using GPS carrier-phase data from the reference stations. As shown in Figure 3, the ionosphere is divided into three-dimensional cells in a sun-fixed reference frame, or "local time/geodetic latitude" (cell size of 3 × 5 deg, respectively, and height boundaries at 60–740–1420 km). In these cells, it is assumed that the electron density is constant during the filter batch. Let L1 = λ_1 ϕ_1 (where λ1 is the wavelength

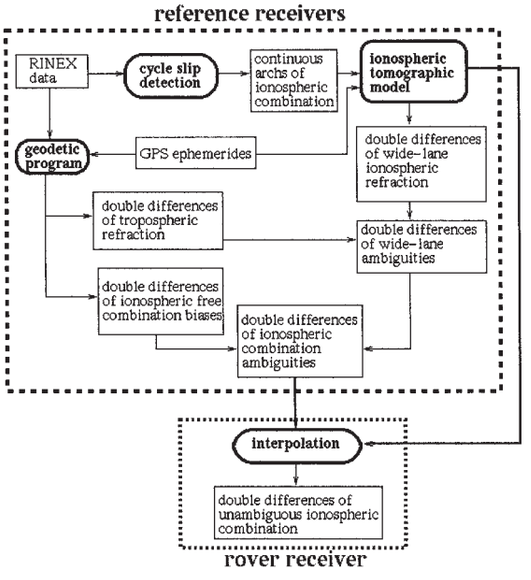

Fig. 2–Flow Chart of Ionospheric Correction Procedure

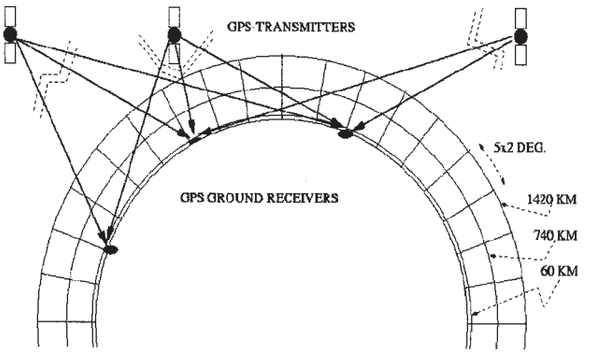

Fig. 3–Layout of the Two-Layer Tomographic Model Adopted to Estimate the Electron Content from Reference Ground Stations

and ϕ_1 the phase corresponding to the L1 frequency), and L2 = λ_2 ϕ_2 (for the L2 frequency).

Then for each pair satellite–receiver, the frequency dependence of the radio-wave propagation delays in the ionosphere provides the following equations for the phase ionospheric combination LI = L1 − L2, proportional to the Slant TEC, or STEC:

$$LI \approx \sum_i \sum_j \sum_k (N_e)_{i,j,k} \Delta s_{i,j,k} + \lambda_1 b_1 - \lambda_2 b_2$$

where i,j,k are the indices for each cell corresponding to local time, geodetic latitude, and height, respectively; $(N_e)_{i,j,k}$ is the corresponding free electron density; and $\Delta s_{i,j,k}$ is the length of the ray path crossing the i,j,k cell ($\Delta s_{i,j,k}$ = 0 for "dark" cells). Finally, the b_1,b_2 are the ambiguity terms, associated with wavelengths λ_1 and λ_2, respectively, including the instrumental delays.

Similar equations can be written for the ionospheric observable PI = P2 − P1, based on the pseudorange P1, P2 measurements. Then the transmitter and receiver code instrumental delays D^T and D_R appear, instead of the ambiguity terms.

Estimating the electron density $(N_e)_{i,j,k}$ from the dual-frequency measurements is an inverse problem. The parameters of the two-layer model are obtained using a Kalman filter with 6–10 min data batch intervals, and assuming the following stochastic behavior for the process noise:

Electron density N_e: random walk with spectral density
$dQ/dt = 10^{10}$ (electrons/m^3)/h

in the above-mentioned solar-fixed reference frame.

Instrumental delays D^T and D_R: constants
Ambiguities $\lambda_1 b_1 - \lambda_2 b_2$: constant along each arc of continuous data phase and white noise in the cycle slips

The electron density in the model can be estimated with only carrier-phase data, but the introduction of

code data (with an appropriate weight $\sigma_{p1} = 100\sigma_{L1}$) provides more strength in the estimation of phase ambiguities, and allows estimation of the instrumental delays. After the filter initialization, the solution is driven mainly by the phase data, and hence is practically immune to Anti-Spoofing and code multipath. This represents an additional improvement over methods that use pre-aligned phases with the code, or smoothed codes.

Step 2—The unambiguous ionosphere at fixed sites is found with help from a geodetic program. The coordinates of the permanent control stations are already known at the centimeter level in a well-defined reference frame. One can use a geodetic GPS data analysis program (in this case, GIPSY) to estimate, with centimeter precision, the biases in the ionosphere-free linear combination (Lc) of L1 and L2 and the residual tropospheric refraction that remains after correcting with a standard atmosphere model. Then one can compute accurate geometric ranges between stations and satellites, corrected for the troposphere and the ionosphere (using the ionospheric model). For distances of a few hundred kilometers, errors in the broadcast ephemeris can be safely ignored at this stage.

Since the control stations operate continuously, it is possible to estimate continuously the ionospheric model, the Lc biases, and the tropospheric refraction. When a rover receiver starts to operate, many of these control station quantities should have well-converged sequential estimates ready for immediate use.

The wide-lane ambiguities are found by rounding off the differences between wide-lane and refraction-corrected geometric range. It is critical that the combined range error and wide-lane noise be less than 43 cm, or half a wide-lane wavelength. One important factor limiting the accuracy of the ionospheric correction is low satellite elevation. Tests conducted to date suggest the ionospheric corrections can be used safely down to almost 20 deg elevation.

From the centimeter-level estimated biases of the ionospheric-free combinations b_{Lc} and the resolved wide-lane ambiguities N_w (double differenced) it is possible to obtain the L1, L2 ambiguities N1 and N2. The relevant equations are:

$$\begin{aligned} b_{Lc} &= 0.5\,[\lambda_\omega N_w + \lambda_\nu (N1 + N2)], \text{ so} \\ N1 + N2 &= \text{nearest integer}[(2\,b_{Lc} - \lambda_\omega N_w)/\lambda_\nu] \\ N1 &= 0.5\,[N_w + (N1 + N2)] \\ N2 &= N1 - N_w \end{aligned}$$

where $\lambda_\omega \approx 86$ cm, $\lambda_\nu \approx 11$ cm, are the wavelengths of the wide and narrow lanes, respectively.

Finally, one finds the unambiguous double-differenced ionospheric STEC: $LI = L1 - L2 - (\lambda_1 N_1 - \lambda_2 N_2)$ for the control stations.

Step 3—Interpolation is performed. To find the ionospheric correction for the rover, we take the unambiguous double-differenced ionospheric STEC, or LI, calculated in step 2 for the baselines between reference stations, and interpolate it to a baseline between the rover and any reference station. For the one test discussed in detail in this paper, the linear interpolation of the unambiguous LI was used, as in [2].

RESOLVING AMBIGUITIES ON THE FLY IN THE KINEMATIC SOLUTION FOR THE ROVER

To resolve ambiguities OTF, the user first combines rover data with information received from the network over a radio or telephone link, forming ionosphere-corrected double differences between the rover and some network stations. The OTF algorithm illustrated in flow-chart form in Figure 4 is then used, in two main steps.

Step 1—Resolving the wide-lane ambiguity. All Lc biases are continuously floated (estimated as real-valued unknown constants) in the navigation filter as part of the kinematic solution, along with the position of the rover, orbit errors, and tropospheric model errors. The rover position, in general, cannot be expected to be known as well as the positions of the stations. This is one reason for the different treatment

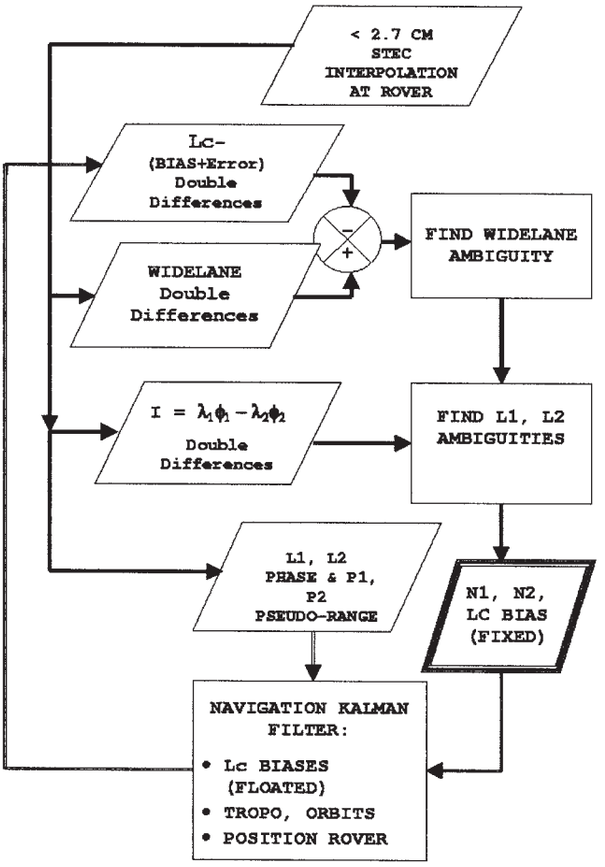

Fig. 4–Flow Chart of the OTF Algorithm for Resolving the L1, L2 Ambiguities in Order to Position the Rover (parallelograms = data; rectangles = operations on data)

of rover and stations. (Biases that are not fixed, for whatever reason, default to their floated values, so there may always be a solution.) In real time, a Kalman filter is used to obtain a joint solution for the present rover coordinates and all the other unknowns (in postprocessing, one would use a smoother as well). The data are the dual-frequency carrier phase and pseudorange.

The double-differenced ambiguous wide lane is first corrected for the ionosphere, using the interpolated model. Then, the ionosphere-free combination Lc, corrected with the current estimate of its floated Lc bias, is subtracted from the wide lane. This is repeated for every double difference for which there is a reliable ionospheric correction (satellites above 20 deg in elevation).

The result of this operation is the wide-lane ambiguity (in meters), plus carrier-phase noise, minus the error in the ionospheric correction and in the estimated Lc bias:

$$\lambda_w N_w + \text{noise(wide lane)} - \text{error(ionospheric} + \text{Lc bias)} = \text{wide lane} - \text{Lc} - \text{ion. correction} - \text{estimated Lc bias}$$

The wide-lane ambiguity, N_w, can be found by rounding off this result to the nearest integer number of wide-lane wavelengths. Errors in computed tropospheric refraction, reference station coordinates, and satellite ephemeris cancel out when Lc is subtracted from the wide lane. Assuming the ionospheric correction is sufficiently accurate to resolve the L1 and L2 ambiguities (better than 2.7 cm, or a half-cycle of the LI ambiguity, as in step 2 below), the main uncertainty is in the estimated Lc bias. Assuming further that the main sources of uncertainty are normally distributed, the error in the Lc bias should be less than one-quarter of a wide lane ($<$21.5 cm) for the procedure to work about 95 percent of the time.

Step 2—Resolving the L1 and L2 ambiguities. Once the wide-lane integer ambiguity N_w is known, one can exploit the following relationship, which the corrected but still ambiguous STEC LI = L1 − L2 and its error must satisfy together:

$$\text{LI} - N_1(\lambda_1 - \lambda_2) - N_w\lambda_2 - \text{ionospheric correction for LI} = \text{noise (LI)} + \text{error (ionospheric correction for LI)}$$

From this it follows that

$$N_1 = \text{nearest integer } [(\text{LI} - N_w\lambda_2)/(\lambda_1 - \lambda_2)]$$

as long as the sum of noise and ionospheric correction error in LI is less than a half-cycle of LI, or $\frac{1}{2}\,|\lambda_1 - \lambda_2|$, or 2.7 cm. Finally:

$$N_2 = N_1 - N_w$$

Once N_1 and N_2 have been found, the exact Lc bias can be calculated and assimilated in the Kalman filter as an additional (pseudo) observation. Since the filter is of the usual covariance type, some "noise" uncertainty must be assigned to every observation. By trial and error, σ = 3 cm has been found to be a conveniently small standard deviation for that noise.

The geometry-free procedure outlined above does not require an integer search as long as the various uncertainties are smaller than the specified bounds. In particular, the effect of the data noise and of the instantaneous LI correction errors has been reduced by using data averages. By trial and error, a data-averaging interval of 2 min has been selected (this is also the data compression interval of the kinematic navigation procedure outlined at the end of this section). Generally speaking, it takes about 6 min of assimilating data before the navigation filter can produce Lc bias estimates precise enough to resolve the wide lane. (For faster resolution, an integer search could be added to the procedure.)

Candidate integer values for the ambiguities are used or rejected as follows. No pair of L1, L2 ambiguities is considered resolved unless the absolute value of the residual STEC LI, after the data have been corrected with the interpolated model and the LI ambiguity has been resolved, is less than 2.7 cm.

Resolved Lc biases are not deemed acceptable unless they pass a null-hypothesis test of their differences from their floated values. And only those floated Lc biases known with worse than 3 cm (formal) precision are replaced with their resolved values via a filter update. (The idea is not to take chances "improving" what should be good enough already.)

For the various steps of the method described here, recursive estimation (Kalman filtering) procedures were used, as in an actual real-time application. The corresponding software is described briefly below.

The tomographic ionosphere model was computed with software from the Group of Astronomy and Geomatics, Universitat Politènica de Catalunya (gAGE/UPC), written by the last three authors. GIPSY was used for the geodetic calculations needed to resolved the fixed-site ambiguities. All this software runs on a PC under Linux. The navigation solution, including estimation of the floated Lc biases, GPS broadcast orbit errors, and tropospheric correction errors (residual zenith delays), was computed using the "IT" software developed by the first author. This software, used for precise, long-range kinematic and static positioning [17–19], was modified for this study so as to make use of the ionospheric corrections. Written in Fortran, it runs under Windows 98, NT, and 2000; Linux; FreeBSD; and Unix. It has been used repeatedly to calculate kinematic position with subdecimeter precision over baselines of more than 1000 km.

All the unknowns required for the present work are included in the observation equations and filter

dynamics: as constants (the Lc biases and the initial orbit states), as random walks (the residual zenith delays and the unmodeled orbit accelerations), and as zero-memory states (the rover coordinates). The calculation also gives the likely precision of each estimated Lc bias, which is needed to decide whether this estimate is good enough for resolving the wide-lane ambiguity. One characteristic of this kinematic technique is the use of data compression (averaging both data and observation equations over periods of several minutes) to reduce the number of filter updates and speed up computation. Experience has shown that 2 min is a good compression interval. Having data compression already implemented in the navigation filter makes it easy to use averages of both data and ionospheric corrections to improve the reliability of the OTF algorithm.

Timed in an older Pentium II PC, each instantaneous position fix takes less than 0.05 s, and every full filter update (once every compression interval) some 0.1–0.2 s. The total time needed at every epoch for all the various calculations by both network operators and users is a small fraction of a second, even with our rather outdated PCs.

TESTING THE PROCEDURE

Since 1999, a series of tests has been performed in different parts of the world under progressively more rigorous conditions. The tests have taken place over larger areas, with longer distances between receivers, and with increasing ionospheric activity as the current solar cycle has peaked. This section provides an overview of those tests, followed by a detailed description of the results of one test. Table 1 lists for each test the epoch, prevailing level of ionospheric activity, distance from the rover to the nearest base station, type of rover, overall percentage of successfully resolved L1,L2 ambiguities, and publications describing each test in detail (identified by their reference numbers in this paper). The reference sites used in each test either belong to a regional network collecting 1 s data for the test or are International GPS Service (IGS) sites with 30 s RINEX data files freely available on the Internet. There are two types of "rover": (1) an actual vehicle (GPS data available every second), and (2) an IGS site (data available every 30 s) or a site specially set up (data every second). In the first case, an auxiliary receiver, never more than a few kilometers away from the vehicle, is used as a base station for deriving a precise, short-baseline kinematic solution, used as "truth" for checking the wide area results. In the second case, the known coordinates of the fixed site chosen as "rover" fulfill the same purpose.

In two of the tests, the data for the rover were also used in calculating ionospheric corrections; in the other tests (such as the one presented in more detail in the next section), they were not. In the Asia/Indian Ocean Test (in a tropical region spanning both northern and southern Appleton ionospheric anomalies), the tomographic model was validated over the ocean by comparing its predicted values with those measured with the dual-frequency altimeter of the TOPEX/POSEIDON satellite [21]. No receiver was treated as the "rover" in this study, and the ionosphere model was tested resolving ambiguities for the network sites only.

PACIFIC NORTHWEST TRIAL

The data used for this study were collected at five North American reference stations belonging to the IGS on 3 May 1998 from 20 to 23 h Universal Coordinated Time (UTC) during high ionospheric

Table 1 — Summary of Test Results

Ref. No.	Ionospheric Activity	Baseline lengths (km)	Probable Success for rover > 80%?	Type of Rover	Rover Data in Model?	Epoch (mmddyy)	Region
11	Quiet (Kp < 4)	116/286	Yes	Both a fixed site and a car	No	03–23–99	Spain
13, 14	Active (Kp > 4)	300/900	Yes	IGS site	No	05–03–98	North America
15	Solar max.	130/500	Yes	IGS site	No	04–19–00/ 04–22–00	Central Europe
20	Fast-changing	162/900	Yes	IGS site	No	04–28–98/ 05–01–98	North America
20	Solar max. very active	130/500	Yes	IGS site	No	07–12–00/ 07–15–00	Central Europe
21	TIDs	144/285	Yes	Fixed site	Yes	08–25–99	Baltic Sea
16, 21	Variable (Kp 0–9)	1000/3000	No rover > 80% for stations	NA	NA	03–06–01/ 04–02–01	SE Asia/ Indian Ocean

Note: TID = traveling ionospheric disturbance (a large wave-like perturbation); NA = not applicable.

activity (Kp >4), followed by a period of geomagnetic storm conditions (Kp >8) during which few useful measurements were available. Figure 5 shows the Kp for May 2, 3, and 4.

The baselines ranged from 300 to 900 km in length, as shown in Figure 6. All observations were dual-frequency carrier-phase and pseudorange, collected at the typical IGS rate of 30 s. Datasets from four of the sites (CABL, GWEN, HOLB, and WILL) were used to create the ionospheric model. Data from all five sites (those mentioned, plus ALBH, near Victoria, in Vancouver Island) were used in the tests described below. ALBH was used as "rover," and the other four as wide area reference sites.

ALBH was positioned relative to HOLB (acting as the base station), some 400 km away. The site closest to ALBH was GWEN, 330 km away, so that was the minimum distance involved in the interpolation of the ionospheric model. While all data had been collected before we carried out our calculations, we took care to process them as they would be during an actual real-time application.

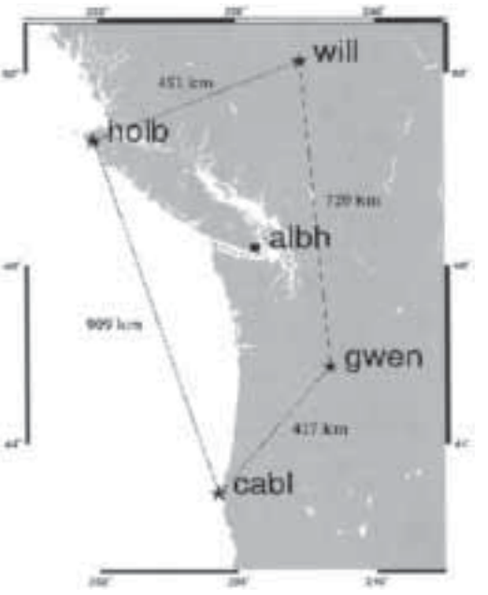

Fig. 6–IGS Sites used in the Pacific Northwest Test

TEST RESULTS

Checking the Ionospheric Corrections Against the Known STEC at ALBH

The differences between the true and the interpolated STEC at ALBH show a root mean square (RMS) of 9 cm (approximately 0.9 TECU) in $L_1 - L_2$ delay units. Thus they have an effect on the wide lane of less than a half-cycle, allowing successful resolution of most wide-lane ambiguities.

The ALBH data have been reserved for ionospheric and kinematic testing. The actual double differences of STEC at ALBH are to be compared with their tomographic predictions (see map in Figure 6). The L1, L2 ambiguities of the carrier phase, double differenced relative to HOLB, are to be resolved OTF, as part of a kinematic solution in which the station is treated as the "rover" (with HOLB as base station).

More than 90 percent of successful wide-lane fixing is obtained for elevations greater than 20 deg, rising to 100 percent if pseudorandom number (PRN) 10 is excluded, in contrast with the minimum elevation of 50 deg when the double-differenced ionospheric correction is neglected (Figure 7). The signals from PRN 10, most of them at low elevation, illuminate a part of the ionosphere to the south not sounded with other satellites. The consequence—poor determination of the ion content in that location—could be avoided by extending the area with more reference stations.

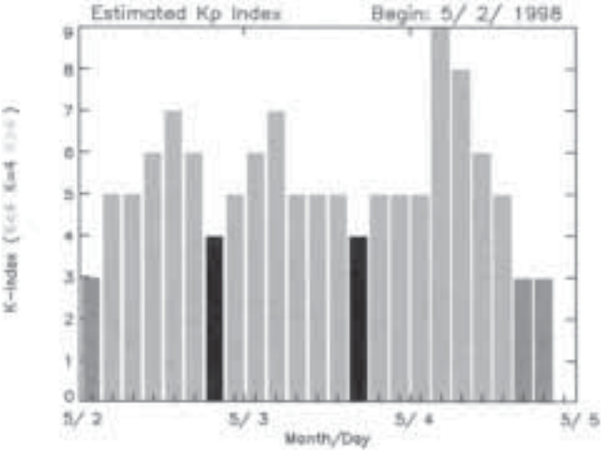

Fig. 5–Geomagnetic Activity During Test, as Indicated by the Planetary Kp Index (Note the elevated value [> 4]. UTC time. Plot from National Oceanic and Atmospheric Administration's Space Environment Center.)

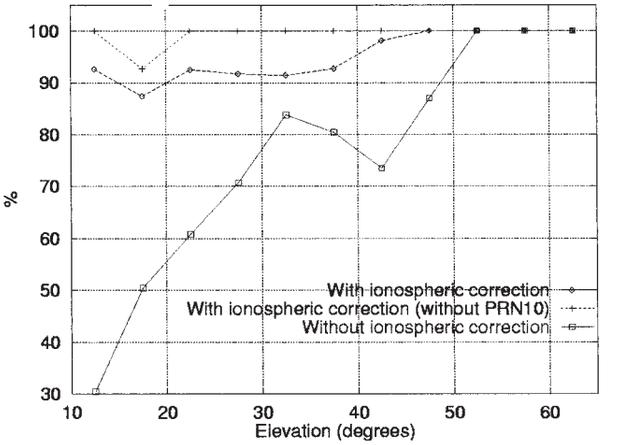

Fig. 7–Percentage of Successful Double-Differenced Wide-Lane Integer Ambiguity Determination as a Function of the Lowest Satellite Elevation

After processing of 6 h of data from the fixed stations, the determination of the ionospheric TEC and residual tropospheric delay have converged sufficiently. Over the next 6 h, the ionospheric effect on the signals from most satellites has been estimated within 10 min of the satellites' rising above the elevation cutoff, with sufficient precision to resolve the wide-lane ambiguity.

Given that the station coordinates are known very precisely, the Lc bias can be determined to better than 3 cm in 2–4 min. Thus by the time the wide lane has been resolved, the Lc bias is already known well enough to resolve most of the L1, L2 double-differenced ambiguities between the network stations.

Interpolating to the test site (ALBH) the unambiguous STEC values double differenced between HOLB and the other stations, it is posible to correct the data for the ALBH–HOLB baseline for refraction and resolve first the STEC and then the L1 and L2 ambiguities, and so the Lc biases, if the interpolation is better than 2.7 cm in accuracy (the difference between interpolated and actual values). This happens 80–100 percent of the time for the test baseline ALBH–HOLB (Figures 8 and 9). The common reference satellite used in forming the double differences (PRN 30) is at a low elevation in the last part of the period (near 20 deg), which coincides with the worst results, between 22.5 and 23 (UTC).

Resolving the L1 and L2 Ambiguities on the Fly for the "Rover" (ALBH)

In the second part of the test, the instantaneous position of ALBH relative to HOLB, 420 km away and on the opposite end of Vancouver Island, was calculated kinematically and then compared with the precisely known position of ALBH, after taking the effect of the solid-earth tide into account.

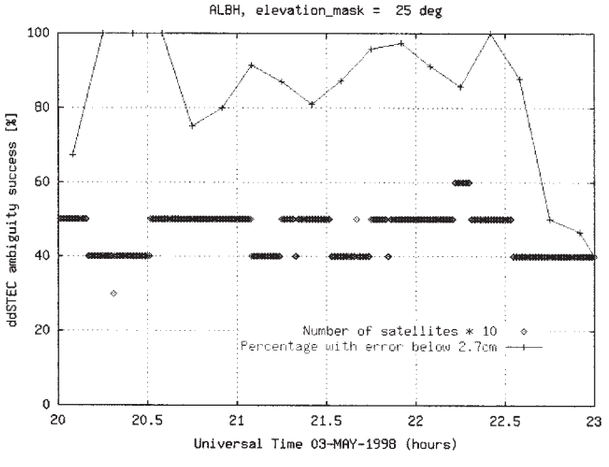

Fig. 8–Percentage of Successful Determination of the Double-Differenced STEC Ambiguity (i.e., correction within 2.7 cm of the true value) for "Rover" Site ALBH and Number of Satellites at More Than 25 deg Elevation

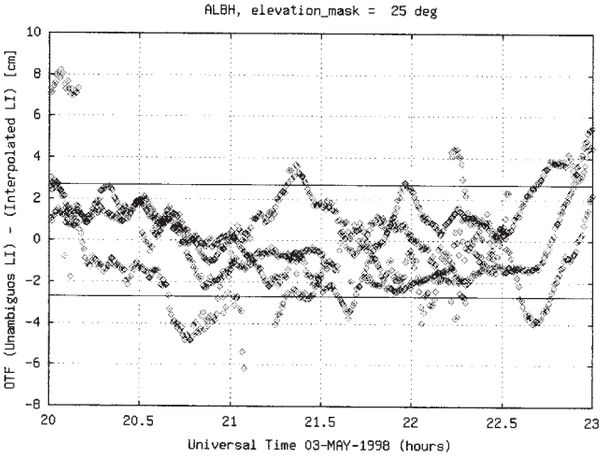

Fig. 9–Possible Ionospheric Correction Errors (interpolated minus measured values, in cm of STEC delay; successful L1, L2 ambiguity resolution is to be expected when these differences are within +/– 2.7 cm)

Solutions were derived with (1) precise IGS ephemeris (from SP3 orbit files), and (2) broadcast ephemerides (from the GPS navigation message). In both cases, the L1 and L2 ambiguities were found OTF using the ionospheric corrections with the OTF technique discussed earlier (Figure 4). The actual position of ALBH was known with centimeter-level precision from an independent IGS solution, after taking into account the solid-earth tidal displacement. This information was not used, in deriving the kinematic solutions, only in testing their accuracy. When the broadcast ephemerides were used, their errors were estimated and corrected as part of the kinematic solution, along with tropospheric refraction correction errors, the floated Lc biases, and the position of the vehicle, using the long-baseline procedure described in [18].

The a priori 1 σ uncertainties were 10 m for Lc biases (using the difference between phase and pseudorange as an initial guess), and 100 m per coordinate for the vehicle. These coordinates were treated as zero-memory or white-noise error states, with no dynamic constraints on the vehicle.

Each OTF solution was tested in two ways. The first involved finding the discrepancies between the known coordinates and the kinematic position of ALBH. Since the resolved ambiguities were used only when needed, this first test covered only attempts to resolve ambiguities obtained soon after gaining or regaining lock (mainly at the start of the run). The resulting up (height), east, and north discrepancies—dUp, dE, and dN, respectively—are shown in Figures 10–13. Without fixing ambiguities or correcting the broadcast orbits, the errors reach a size of several decimeters (Figure 10). Adjusting the orbits brings clear improvements (Figure 11). If the ambiguities are fixed as well (Figure 12), the solution achieves decimeter-level accuracy within

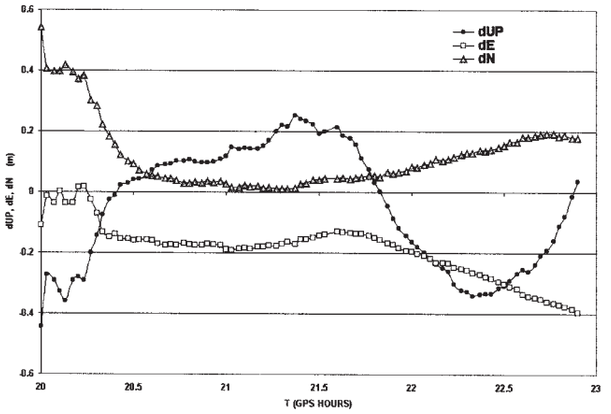

Fig. 10–Kinematic Versus True Position of ALBH, with HOLB as Base Station (a 429 km baseline; broadcast orbits used, but not adjusted; ambiguities "floated" [Lc biases estimated]; tropospheric refraction errors estimated; triangles: dUP, black circles: dN, squares: dE, all in meters)

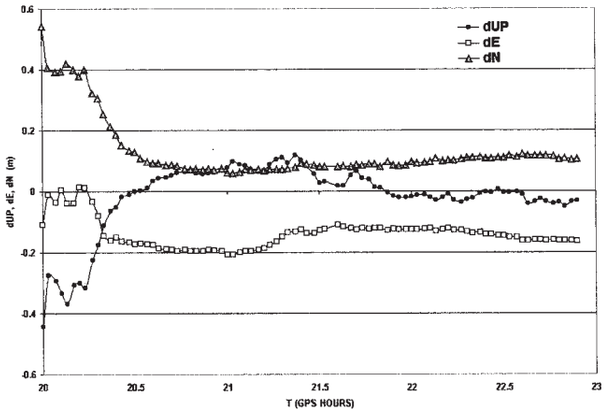

Fig. 11–As in Figure 10, but with the Orbits Adjusted

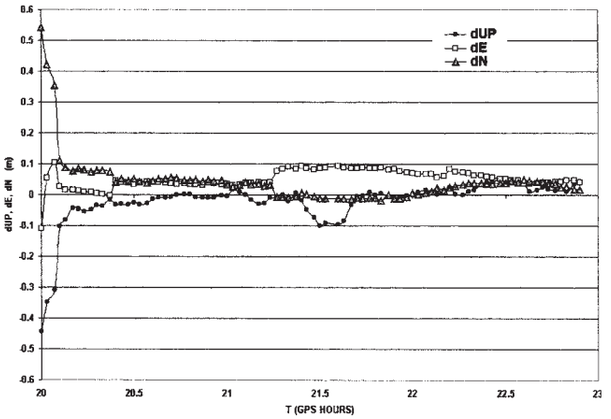

Fig. 12–As in Figure 10, but with Broadcast Orbits Adjusted and Ambiguities Fixed

10 min, when the first three double differences are resolved. That time is down to 8 min when the (fixed) SP3 orbits (Figure 13) are used.

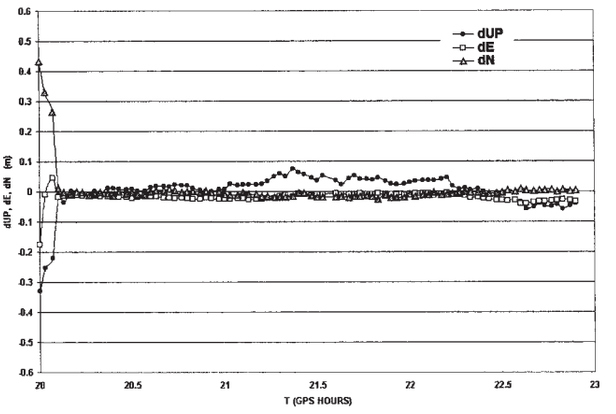

Fig. 13–Same as in Figure 12, but Using Precise SP3 Orbits (from the IGS) Instead of the Broadcast Ephemerides (the SP3 orbits were not adjusted in this run)

The second test of each OTF solution involved comparing all the Lc bias values, Bc, calculated from the resolved N1 and N2 integers (whether or not used in the kinematic solution) with their precise post-processed estimates, Bc*, obtained fixing the coordinates of ALBH and HOLB to their known values and using the precise SP3 orbits from the IGS. The L1, L2 ambiguities can be regarded as successfully resolved if $|Bc - Bc^*| < 2$ cm.

In the 3 h test period, a total of 180 attempts were made to resolve the ambiguities in all ALBH–HOLB double differences with satellites above 25 deg that produced viable candidates (meeting the conditions built into the algorithm). The test criterion was satisfied 71 percent of the time with both the broadcast and the SP3 orbits, but 93 percent of the time when one of the satellites (PRN10) was not counted. This satellite had already been identified by tests at the fixed sites as likely to cause problems. In a real situation, it could be flagged as such in an additional integrity monitoring operation, so users could avoid fixing the ambiguities of double differences associated with it. This issue will be revisited in future studies.

None of the possible errors detected appeared to exceed +/− 1 cycle in both L1 and L2 (the wide lane was always correctly resolved). These errors would affect the Lc biases by +/− 11 cm. Given the frequency with which they occur, their variance is ~5 cm, so one could accommodate them by assigning a standard deviation of 5 cm to all resolved biases.

CONCLUSIONS

After testing the effectiveness of the approach in a number of different situations, we have concluded that real-time ionospheric corrections obtained from computed tomography models can be so precise that most carrier-phase ambiguities can be resolved over

distances of hundred of kilometers between receivers, even at times of considerable ionospheric activity. Our own procedure looks promising, and we hope to improve it. The algorithms outlined in this paper can be implemented in real time. All necessary calculations can be performed with ordinary personal computers. Local area networks have the potential for supporting very precise GPS navigation and surveying work, both in real time and in postprocessing, over areas hundreds of kilometers across and at all stages of the solar cycle.

ACKNOWLEDGMENTS

The authors thank the International GPS Service for making their GPS datasets available. The map shown in this paper was generated with the software package GMT, created by P. Wessel and W. H. F. Smith.

This work was supported in part by the Spanish CICYT TIC-2000-014-P4-03 and TIC-2001-2356-C02-02 projects.

REFERENCES

1. Enge, P., T. Walter, S. Pullen, C. Kee, Y.-C. Chao, and Y.-J. Tsai, *Wide Area Augmentation of the Global Positioning System*, Proceedings of the IEEE, Vol. 84, No. 8, 1996, pp. 1063–1088.
2. Gao, Y., Z. Li, and J. F. McLellan, *Carrier Phase Based Regional Area Differential GPS for Decimeter-Level Positioning and Navigation,* Proceedings of The Institute of Navigation's ION GPS-97, September 1997, pp. 1305–1313.
3. Pratt, M., B. Burke, and P. Misra, *Single-Epoch Integer Ambiguity Resolution with GPS-GLONASS L1-L2 Data*, Proceedings of The Institute of Navigation's ION GPS-98, Nashville, TN, September 1998.
4. Coster, A. J., M. M. Pratt, B. P. Burke, and P. N. Misra, *Characterization of Atmospheric Propagation Errors for DGPS*, Proceedings of The Institute of Navigation's 54th Annual Meeting, Denver, CO, June 1998.
5. Hansen, A. J., T. Walter., and P. Enge, *Ionospheric Correction Using Tomography,* Proceedings of The Institute of Navigation's ION GPS-97, September 1997, pp. 249–257.
6. Hernández-Pajares, M., J. M. Juan, and J. Sanz, *New Approaches in Global Ionospheric Determination Using Ground GPS Data*, Journal of Atmospheric and Solar-Terrestrial Physics, Vol. 61, 1999, pp. 1237–1247.
7. Hernández-Pajares, M., J. M. Juan, J. Sanz, and J. G. Sole, *Global Observation of the Ionospheric Electronic Response to Solar Events Using Ground and LEO GPS Data*, Journal of Geophysical Research-Space Physics, Vol. 103, No. A9, 1998, pp. 20,789–20,796.
8. Howe, B. M., K. Runciman, and J. A. Secan, *Tomography of the Ionosphere: Four-Dimensional Simulations*, Radio Science 33, 1998, pp. 109–128.
9. Mannucci, A. J., B. D. Wilson, D. N. Yuan, C. H. Ho, U. J. Lindqwister, and T. F. Runge, *A Global Mapping Technique for GPS-Derived Ionospheric Total Electron Content Measurements*, Radio Science 33, 1998, pp. 565–582.
10. Liao, X. and Y. Gao, *High-Precision Ionospheric TEC Recovery Using a Regional-Area GPS Network*, Navigation 48, Summer 2001, pp. 101–111.
11. Colombo, O. L., M. Hernández-Pajares, J. M. Juan, J. Sanz, and J. Talaya, *Resolving Carrier-Phase Ambiguities On-the Fly, at More Than 100 km from Nearest Site, with the Help of Ionospheric Tomography*, Proceedings of The Institute of Navigation's ION GPS-99, Nashville, TN, September 1999.
12. Hernández-Pajares M., J. M. Juan, J. Sanz, and O. L. Colombo, *Precise Ionospheric Determination and Its Application to Real-Time GPS Ambiguity Resolution*, Proceedings of The Institute of Navigation's ION GPS-99, Nashville, TN, September 1999.
13. Hernández-Pajares, M., J. M. Juan, J. Sanz, and O. L. Colombo, *Application of Ionospheric Tomography to Real-Time GPS Carrier-Phase Ambiguities Resolution, at Scales of 400–1000 km, with High Geomagnetic Activity*, Geophysical Research Letters, 27, 2009–2012, 2000.
14. Colombo, O. L., M. Hernández-Pajares, J. M. Juan, and J. Sanz, *Ionospheric Tomography Helps Resolve GPS Ambiguities on the Fly at Distances of Hundreds of Kilometers During Increased Geomagnetic Activity,* Proceedings of IEEE PLANS 2000, San Diego, CA, April 2000.
15. Hernández-Pajares, M., J. M. Juan, J. Sanz, O. L. Colombo, and H. Van der Marel, *Real-Time Integrated Water Vapor Determination Using OTF Carrier-Phase Ambiguity Resolution in WADGPS,* Geophysical Research Letters, 28, 2001, pp. 3267–3270.
16. Hernández-Pajares, M., J. M. Juan, J. Sanz, and O. L. Colombo, *Improving the Real-Time Ionospheric Determination from GPS Sites at Very Long Distances over the Equator*, Journal of Geophysical Research—Space Physics (in print).
17. Colombo, O. L., *Errors in Long Distance Kinematic GPS*, Proceedings of The Institute of Navigation's ION GPS-91, Albuquerque, NM, September 1991.
18. Colombo, O. L., *Long Range Kinematic GPS*, in GPS for Geodesy, 2nd Edition, A. Kleusberg and P. Teunissen, eds., Springer-Verlag, 1998.
19. Colombo, O. L. and A. G. Evans, *Testing Decimeter-Level, Kinematic, Differential GPS over Great Distances at Sea and on Land*, Proceedings of The Institute of Navigation's ION GPS-98, Nashville, TN, September 1998.
20. Hernández-Pajares, M., J. M. Juan, J. Sanz, and O. L. Colombo, *Real-Time Integrated Water Vapor Determination Using OTF Carrier-Phase Ambiguity Resolution in WADGPS Networks,* Proceedings of The Institute of Navigation's ION GPS-2000, Salt Lake City, UT, September 2000.
21. Hernández-Pajares, M., J. M. Juan, J. Sanz, and O. L. Colombo, *Tomographic Modelling of GNSS Ionospheric Corrections: Assessment and Real-Time Applications*, Proceedings of The Institute of Navigation's ION GPS-2001, Salt Lake City, UT, September 2001.